

Supporting Information

**Hexamethylenetetramine induced multidimensional defects in Co₂P nanosheets
for efficient alkaline hydrogen evolution**

Tingjuan Wang^a, Chao Wang^a, Yaoyao Ni^a, Yan Zhou^a, and Baoyou Geng^{*,a,b}

^a College of Chemistry and Materials Science, The Key Laboratory of Electrochemical Clean Energy of Anhui Higher Education Institutes, Anhui Provincial Engineering Laboratory for New-Energy Vehicle Battery Energy-Storage Materials, Anhui Normal University, Wuhu, 241002, China.

^b Institute of Energy, Hefei Comprehensive National Science Center, Anhui, Hefei, 230031, China.

Corresponding author: E-mail: bygeng@mail.ahnu.edu.cn

1. Experimental Section

1.1 Raw materials

All materials are purchased commercially without further purification. Cobalt nitrate hexahydrate (AR), Ammonium fluoride (AR), Sodium hypophosphite (AR), potassium hydroxide (AR) are from Aladdin Reagent Co., Ltd. urea (AR) is from Macklin Reagent Co., Ltd. Nickel foam. Hexamethylenetetramine is from Xiya Reagent Co., Ltd.

1.2 Material preparation

Synthesis of $\text{Co(OH)}_2/\text{NF}$

First, the nickel foam was cut into rectangular pieces of 2 x 3 cm² square and then cleaned with acetone, hydrochloric acid, deionized water and ethanol for 15 minutes in turn. It was then placed in a vacuum and dried at 60 °C for 12 hours. 0.1455 g cobalt nitrate hexahydrate was added to 5mL of deionized water for 2 min ultrasonic treatment to ensure full dissolution. 0.5 mL of the above cobalt nitrate solution was diluted with 30 mL of deionized water, followed by the addition of 2 mmol ammonium fluoride and 2.5 mmol urea to obtain a mixed solution. The mixture was stirred for 30 min to ensure uniformity and transferred to a 40 mL Teflon autoclave. Then the pre-treated nickel foam was put into it, and the autoclave was sealed and put into an oven at 120 °C for 10 h. After cooling to room temperature, the nickel form was rinsed with deionized water and ethanol for 3 times respectively. The washed nickel foam was placed in a 60 °C oven and vacuum dried for a whole night to obtain $\text{Co(OH)}_2/\text{NF}$.

Synthesis of $\text{Co(OH)}_2\text{-200HMT}/\text{NF}$

First, a certain amount of HMT (100 mg, 200 mg, 300 mg, 400 mg) was dispersed into 30 mL mixture solvent composed of 27 mL deionized water and 3 mL methanol, and gently stirred for 1 h. Then, the above solution was added to the 40 mL reaction vessel containing the foam nickel precursor prepared in the first step, and reacted at 80 °C for 4 h. After the reaction was completed and cooled to room temperature, the nickel foam loaded with products was washed with deionized water and methanol for three times respectively. The obtained material was dried in a vacuum oven at 60 °C for 12 h to obtain $\text{Co(OH)}_2\text{-HMT}/\text{NF}$. According to the amount of HMT added, the

samples prepared were named as $\text{Co(OH)}_2\text{-100HMT/NF}$, $\text{Co(OH)}_2\text{-300HMT/NF}$ and $\text{Co(OH)}_2\text{-400HMT/NF}$, respectively.

Synthesis of $\text{Co}_2\text{P-200mgHMT/NF}$

The as-prepared $\text{Co(OH)}_2\text{-200HMT/NF}$ was further annealed for the phosphidation reaction with $\text{NaH}_2\text{PO}_2 \cdot \text{H}_2\text{O}$. In a typical synthesis, a piece of $\text{Co(OH)}_2\text{-200HMT/NF}$ was placed in the porcelain boat, and 300 mg $\text{NaH}_2\text{PO}_2 \cdot \text{H}_2\text{O}$ was placed in another porcelain boat. Two porcelain boats were then put into a tube furnace, and the temperature of the tube furnace was set to 350 °C for 2 h. The reaction has taken place in a flow of nitrogen atmosphere, with the heating rate of 2 °C/min. $\text{Co}_2\text{P-100HMT/NF}$, $\text{Co}_2\text{P-300HMT/NF}$ and $\text{Co}_2\text{P-400HMT/NF}$ were obtained when the temperature was reduced to room temperature.

1.3 Material characterization

The morphologies and the sizes of the samples were characterized by scanning electron microscopy (SEM, Hitachi S-4800) and transmission electron microscopy (TEM, Hitachi, HT-7700). The nickel foam loaded with the sample was sonicated for a long time in ethanol solution to make the sample fall off the nickel foam. The ethanol solution containing the sample was dropped on the carbon-coated copper grid for TEM characterization. High-resolution TEM (HRTEM, FEI, Tecnai G2 F30) was used to obtain the information on lattice fringes and high resolution images of materials. X-ray powder (XRD, Bruker AXS, D8 Advance) characterizations were carried out by $\text{Cu K}\alpha$ radiation. Electron Paramagnetic Resonance (EPR) measurements were obtained on the JEOL JESX320 at room temperature. X-ray photoelectron spectroscopy (XPS, Thermo Fisher, ESCALAB 250XI) was selected to analyze the electronic state with the $\text{Al K}\alpha$ monochromatized radiation. The specific surface area and pore size distribution of the material were characterized by an automatic gas adsorption analyzer (McMurray ASAP2010N).

1.4 Electrochemical performance test

Electrocatalytic measurements were actualized by an electrochemical workstation (Chenhua, CHI660C) with the three electrode system in 1.0 M KOH solution at room temperature. The three electrode system is composed of carbon rod electrode as the counter electrode, Ag/AgCl electrode as reference electrode, and nickel foam electrode material ($1 \times 1 \text{cm}^2$) as the working electrode.

The voltages obtained from all experimental data were calibrated by the equation $E_{\text{RHE}} = E_{\text{Ag} / \text{AgCl}} + 0.059 * \text{pH} + 0.197\text{V}$. The scanning rate of LSV curve is 10 mV/s. LSV curves are tested by IR compensation. In the point range outside the Faraday region, the double-layer capacitance (Cdl) is calculated according to the CV curves obtained at different scanning rates (40, 60, 80, 100, 120 mV/s), and the electrochemical active surface area (ESCA) has been estimated. Electrochemical impedance (EIS) tests were carried out in the frequency range from 0.01 Hz to 100 kHz at open circuit voltage. The electrochemical stability of the catalyst material was tested by cyclic voltammetry and chronopotentiometry. The CV cycle range is - 0.4 to - 0.8 V with a scan rate of 10 mV/s.

2. Additional Figures

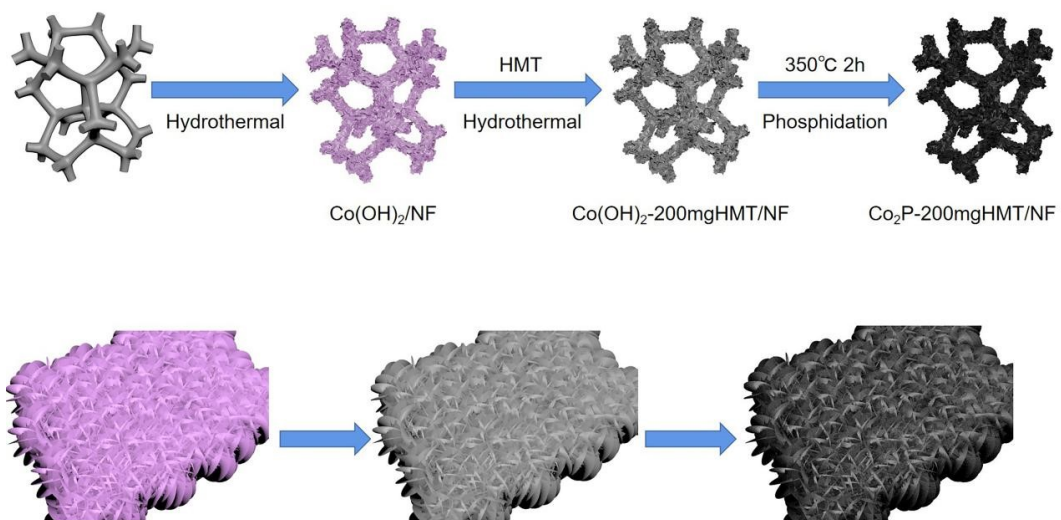


Figure S1. Illustration of the crystal engineering strategy to prepare Co₂P-200HMT/NF Nanosheets.

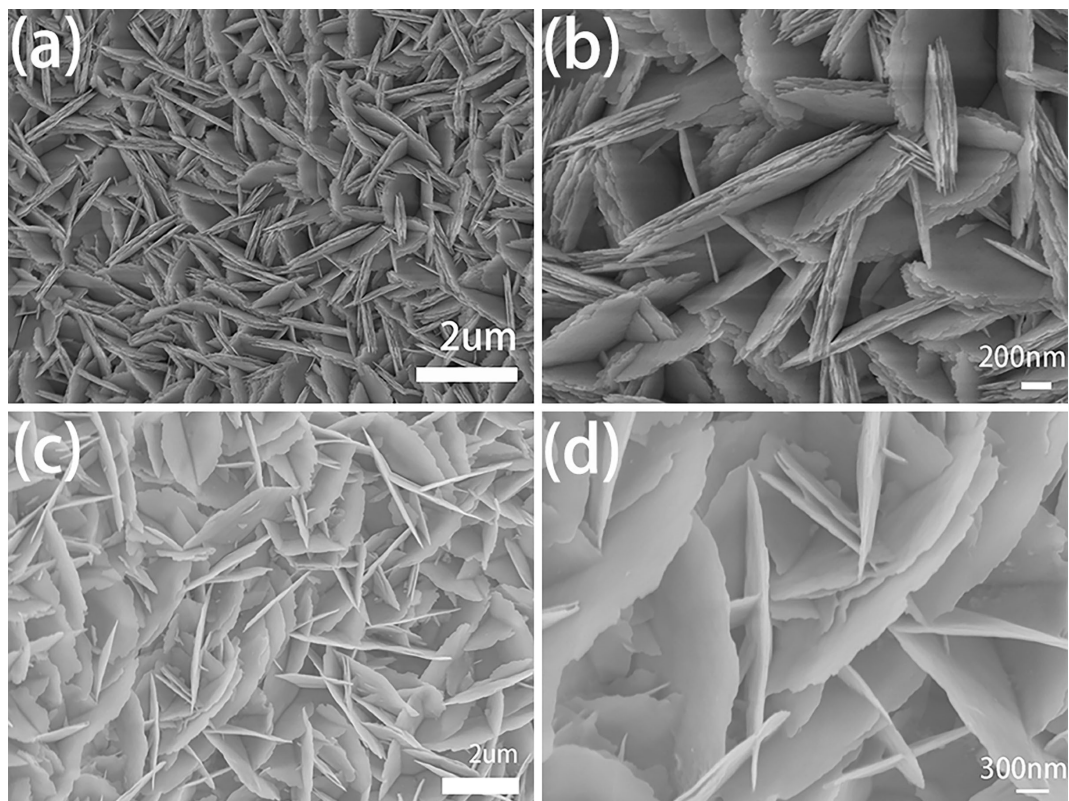


Figure S2. (a, b) SEM images of Co(OH)₂/NF. (c, d) SEM images of Co₂P/NF.

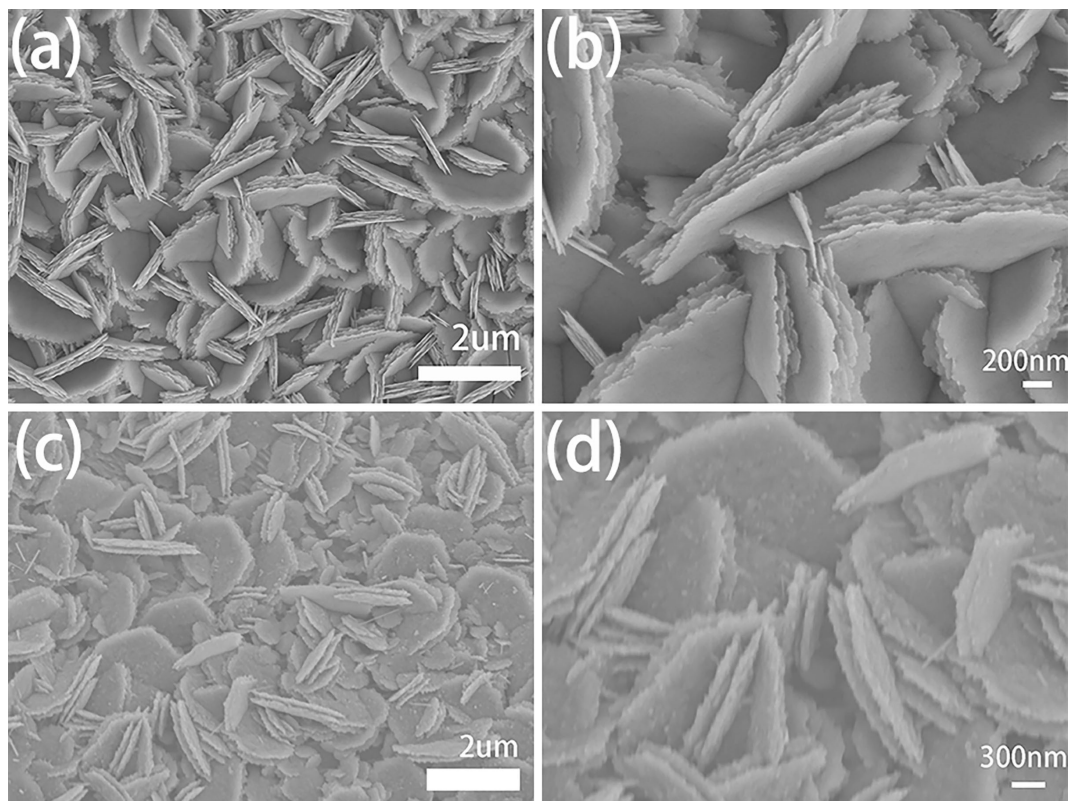


Figure S3. (a, b) SEM images of Co(OH)_2 -100mg HMT/NF. (c, d) SEM images of Co_2P -100mg HMT/NF.

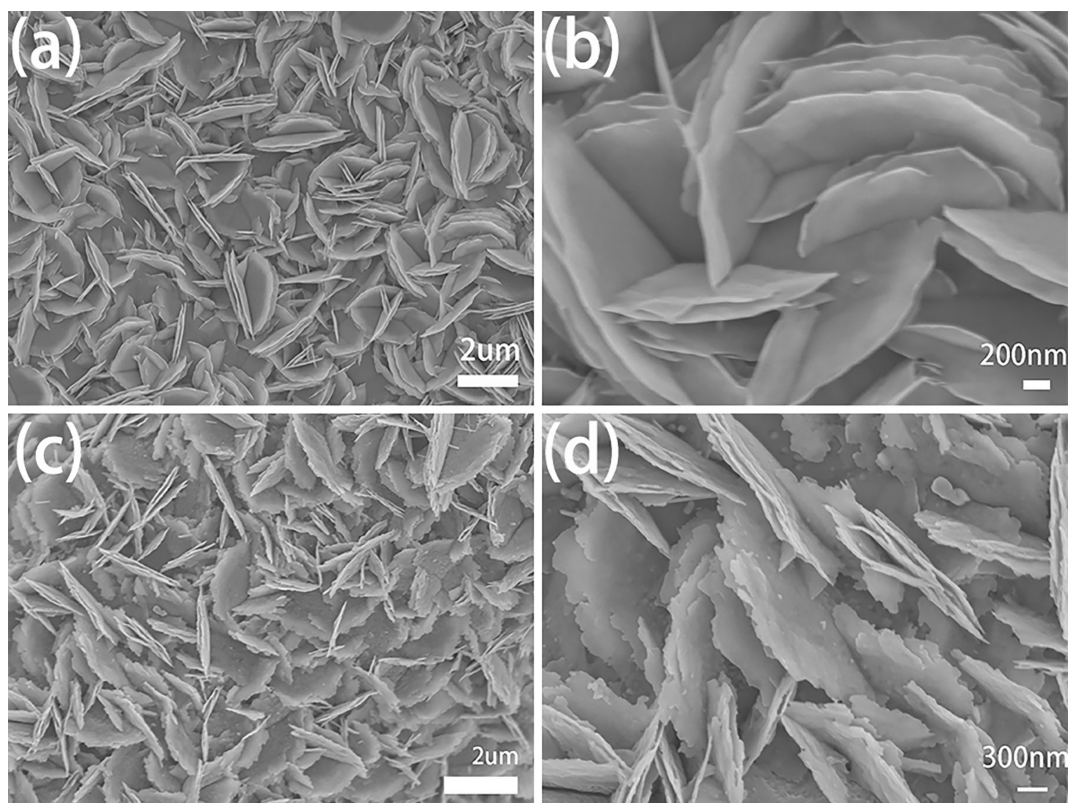


Figure S4. (a, b) SEM images of Co(OH)_2 -200mg HMT/NF. (c, d) SEM images of Co_2P -200mg HMT/NF.

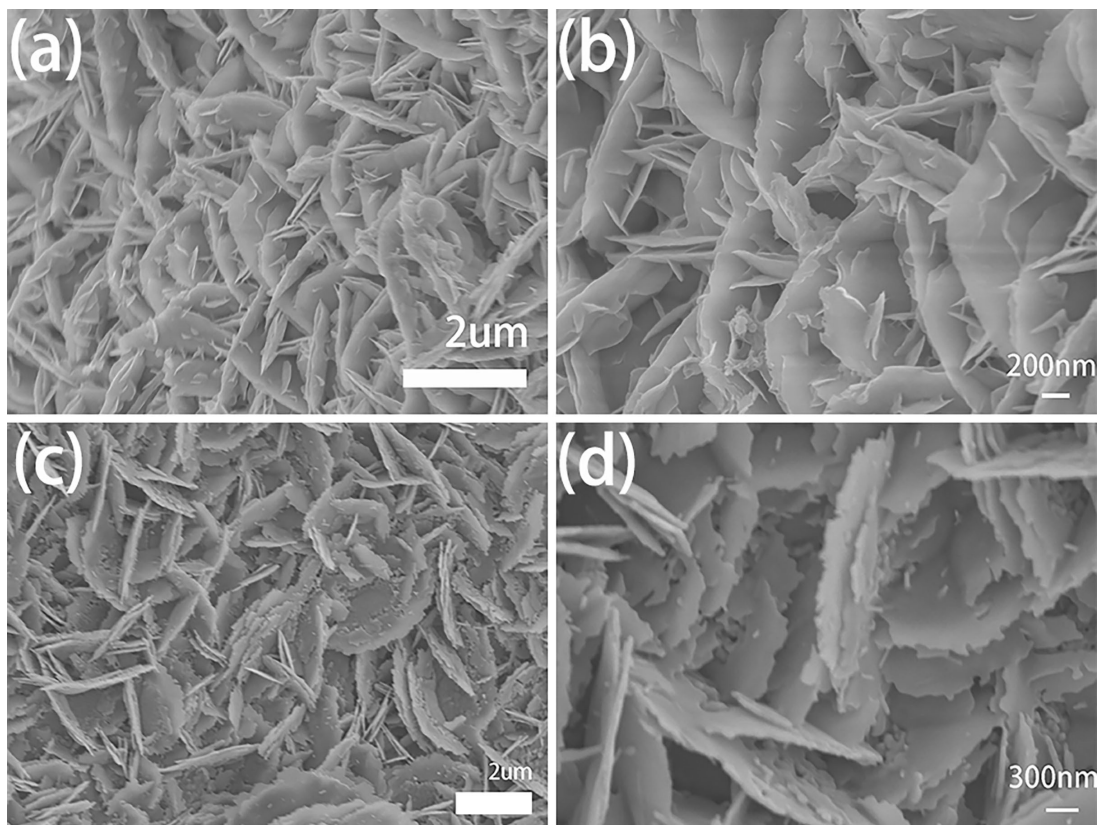


Figure S5. (a, b) SEM images of Co(OH)_2 -300mg HMT/NF. (c, d) SEM images of Co_2P -300mg HMT/NF.

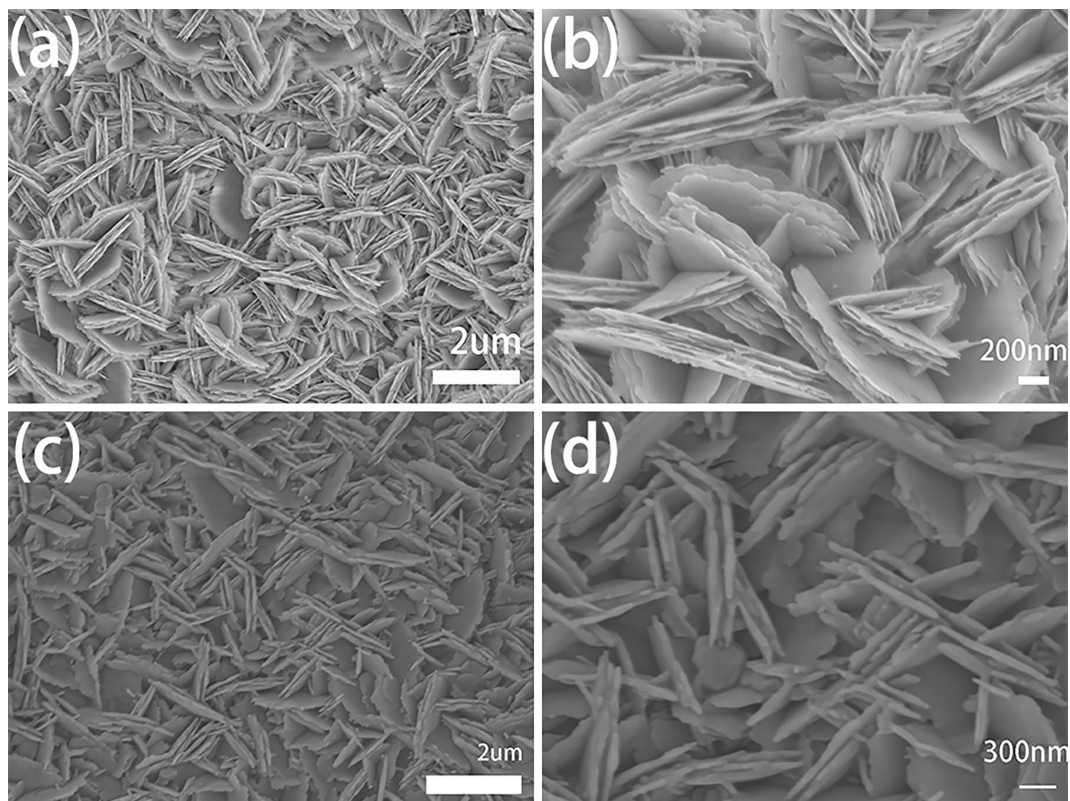


Figure S6. (a, b) SEM images of Co(OH)₂-300mg HMT/NF. (c, d) SEM images of Co₂P-300mg HMT/NF.

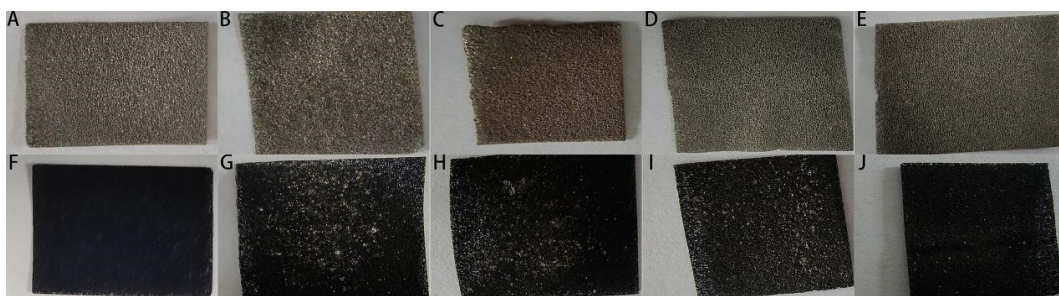


Figure S7. (a-e) Photos of $\text{Co(OH)}_2/\text{NF}$, Co(OH)_2 -100 mg HMT/NF, Co(OH)_2 -200 mg HMT/NF, Co(OH)_2 -300 mg HMT/NF and Co(OH)_2 -400 mg HMT/NF. (f-j) Photos of $\text{Co}_2\text{P}/\text{NF}$, Co_2P -100 mg HMT/NF, Co_2P -200 mg HMT/NF, Co_2P -300 mg HMT/NF and Co_2P -400 mg HMT/NF.

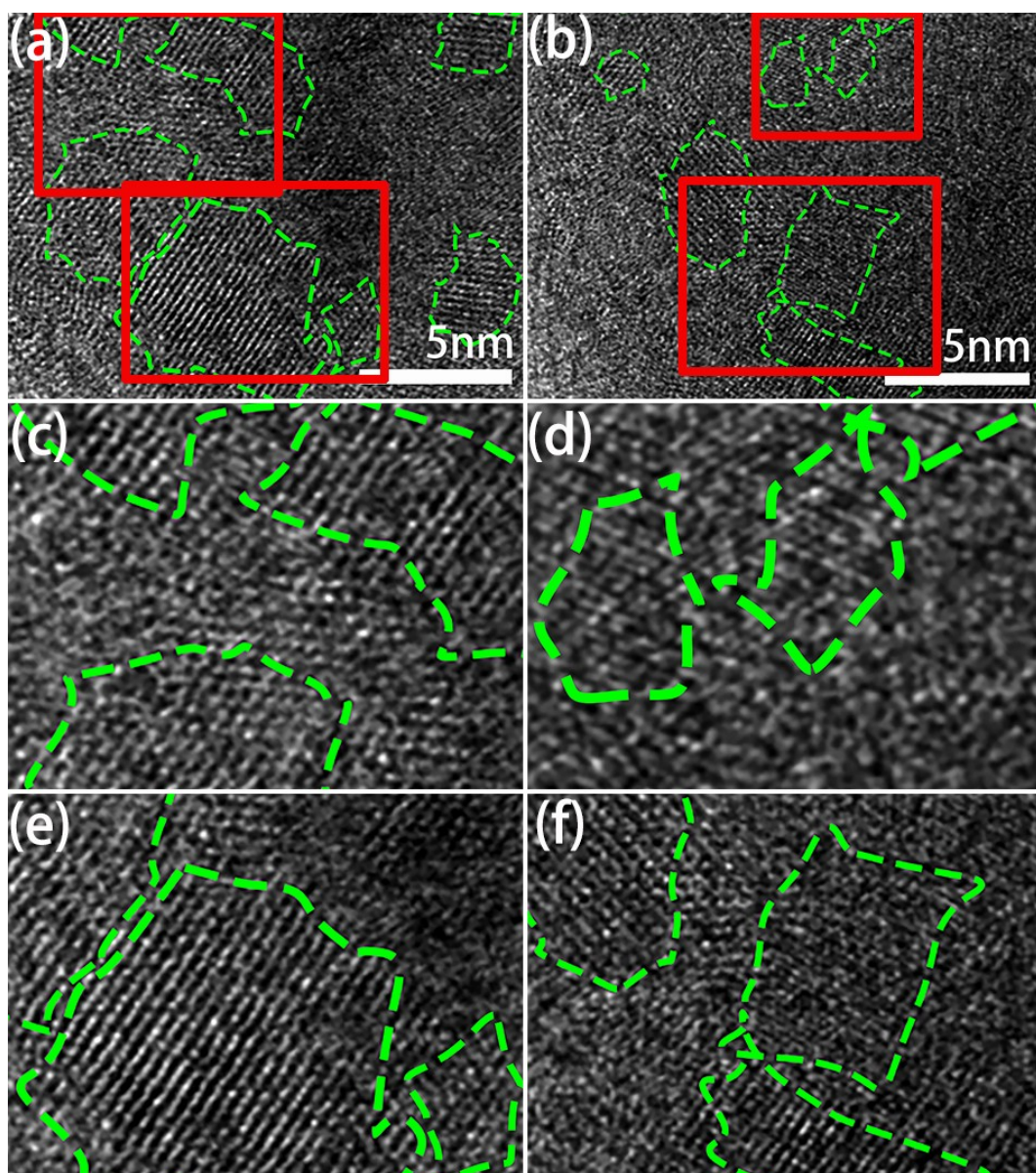


Figure S8. (a, b) The enlarged images of Figure 1f and 1g. (c, d) The larger images of upper red rectangles in (a) and (b). (e, f) The larger images of lower red rectangles in (a) and (b).

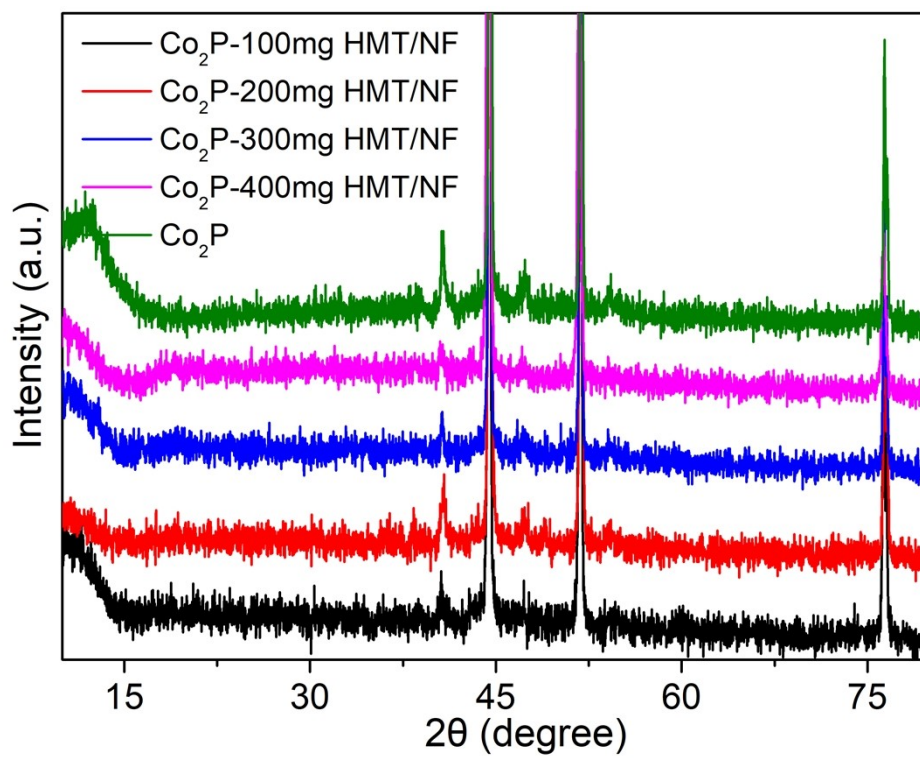


Figure S9. XRD patterns of all samples.

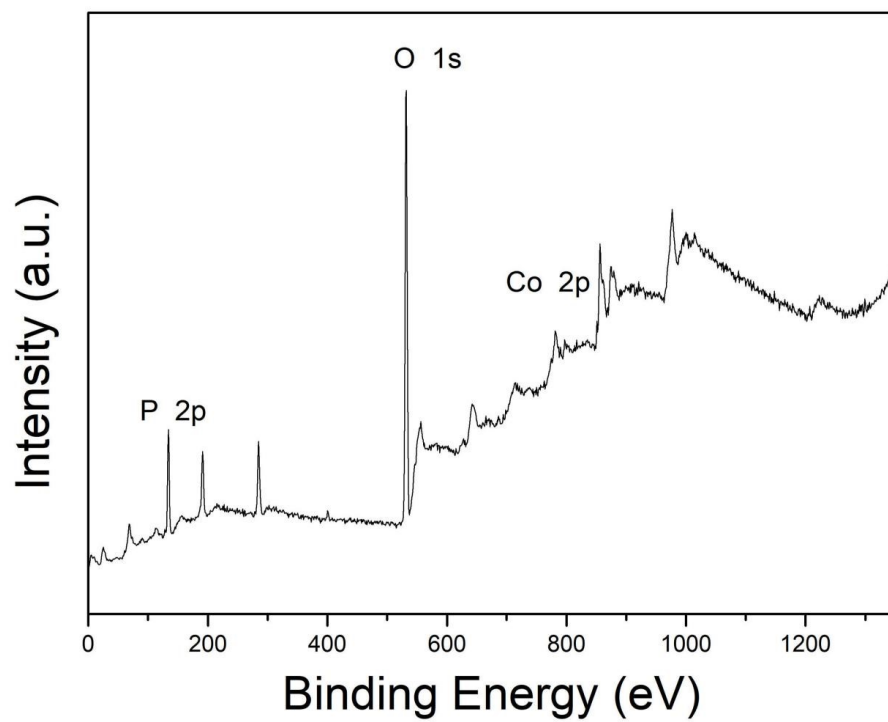


Figure S10. XPS spectrum of Co₂P/NF.

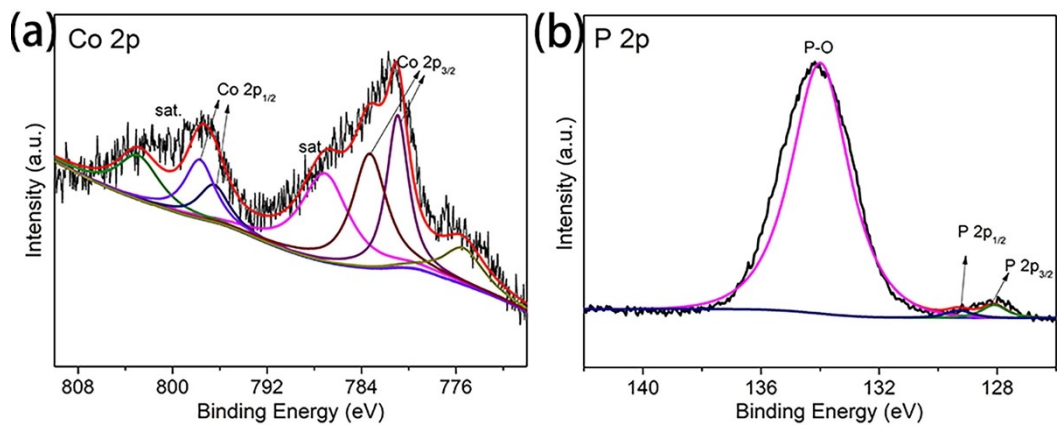


Figure S11. Co 2p (a) and P 2p (b) XPS spectra of $\text{Co}_2\text{P/NF}$.

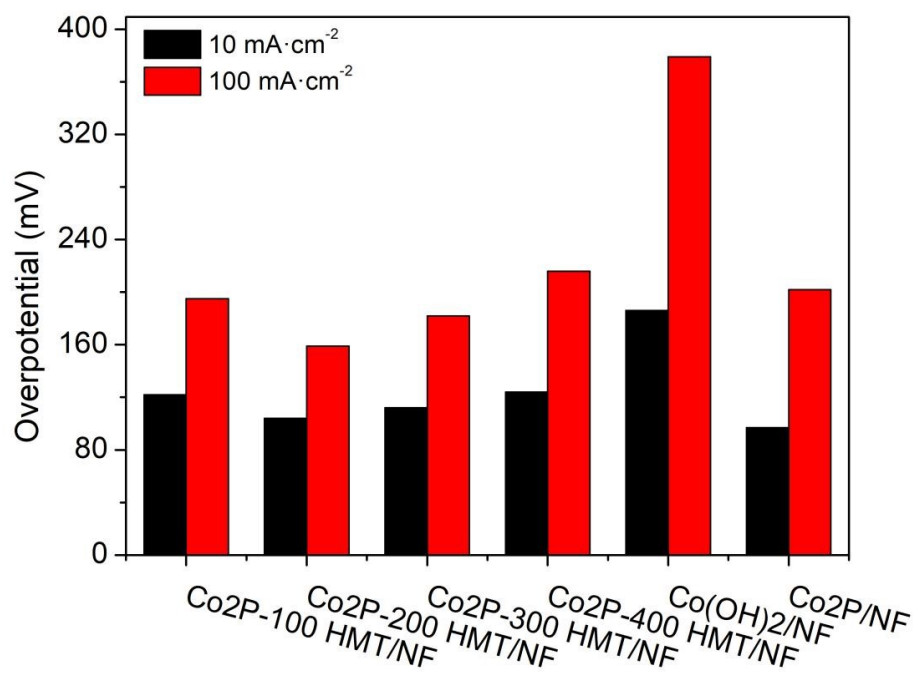


Figure S12. Comparison of over potentials of catalysts at current densities of 10 mA · cm⁻² and 100 mA · cm⁻².

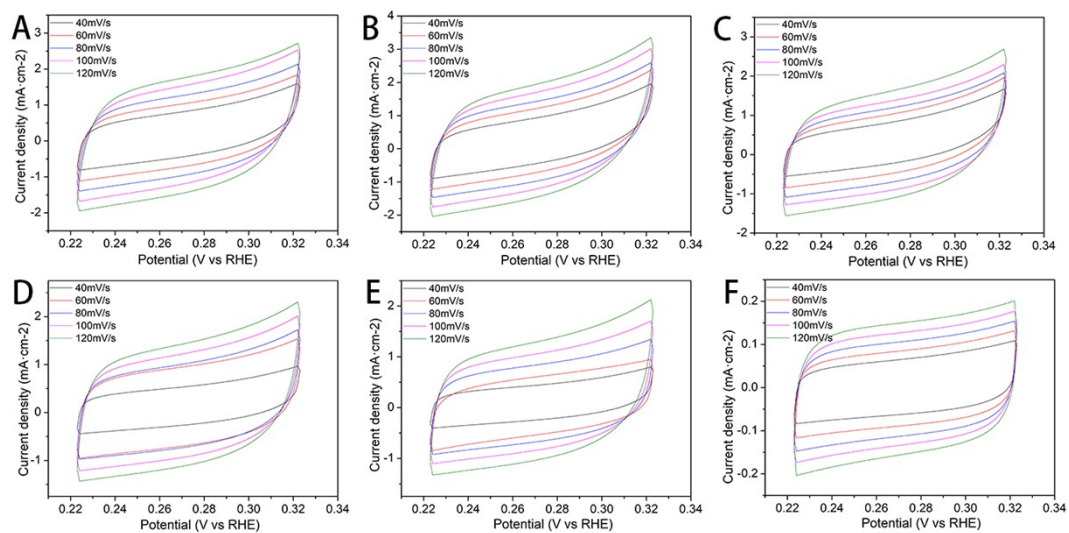


Figure S13. CV curves obtained by scanning from -0.8 v to -0.7 v (vs. RHE) at scanning speeds of 40, 60, 80, 100 and 120 mV/S (a) Co₂P-100 mg HMT/NF, (b) Co₂P-200 mg HMT/NF, (c) Co₂P-300 mg HMT/NF, (d) Co₂P-400 mg HMT/NF, (e) Co₂P/NF and (f) Co(OH)₂/NF.

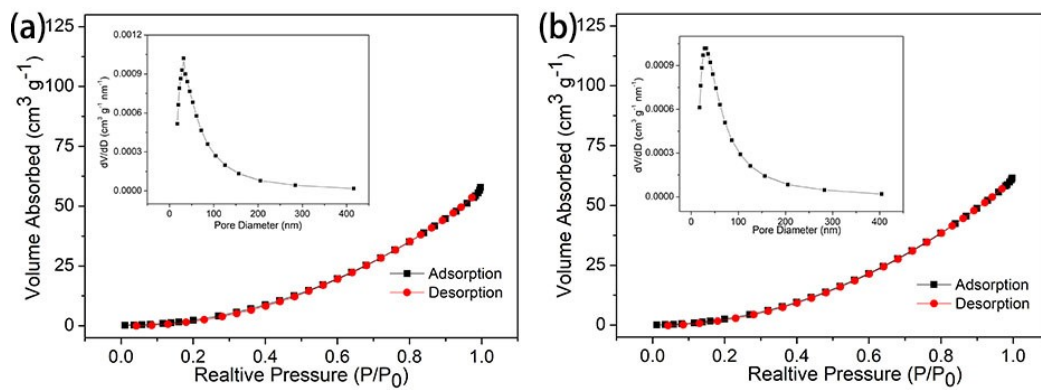


Figure S14. (a) BET specific surface area and pore size distribution of Co₂P/NF. (b) BET specific surface area and pore size distribution of Co₂P-200 mg HMT/NF.

3. Additional Tables

Table S1. The HER activity of the Cobalt based electrocatalysts compared with other recently reported catalysts in the alkaline (1M KOH) medium.

Catalysts	$\eta_{10}(\text{mV})$	$\eta_{100}(\text{mV})$	References
Co₂P-200mg HMT/NF	104	159	This work
Co ₂ P@Cu/NF	99.7	303.2	1
Co ₂ P@Co ₂ P/Co-POM/NF	130	300	2
CoFe-P/NF-1	83	180	3
CoP UNSs/NF	160	252	4
CeO _x /CoP/NF-3	117	260	5
NiFeCoP/NF	/	167.5	6
CoP ₃ /CoMoP-5/NF HNAs	125	/	7
CoMnP/Ni ₂ P/NF	108	/	8
CoxMo1P/NiFe-LDH/NF	98.9	/	9
N-CoO@CoP	/	201	10

References

1. M. R. Yang, Y. Q. Wang, Y. F. Gu, Z. L. Xue, J. H. Shi, W. An, Y. C. Rui, Electro-deposited copper nanoclusters on leaf-shaped cobalt phosphide for boosting hydrogen evolution reaction. *J Alloy Compd* 2022, 902, 163771.
2. L. Zhang, X. Ding, M. Cong, Y. Wang, X. Zhang, Self-adaptive amorphous Co₂P@Co₂P/ Co-polyoxometalate/nickel foam as an effective electrode for electrocatalytic water splitting in alkaline electrolyte. *Int J Hydrog Energy* 2019, 44, 9203–9209.
3. X. D. Wang, C. Wang, F. Y. Lai, H. X. Sun, N. Yu, B. Y. Geng, Self-Supported CoFe-P Nanosheets as a Bifunctional Catalyst for Overall Water Splitting. *ACS Applied Nano Materials* 2022, 4, 12083-12090.
4. Y. Li, F.-M .Li, Y. Zhao, S.-N. Li, J.-H. Zeng, H.-C. Yao, Y. Chen, Iron doped cobalt phosphide ultrathin nanosheets on nickel foam for overall water splitting. *J. Mater. Chem. A* 2019, 7, 20658– 20666.

5. T. Zhang, X. Wu, Y. Fan, C. Shan, B. Wang, H. Xu, Y. Tang, Hollow CeO_x/CoP Heterostructures Using Two-dimensional Co-MOF as Template for Efficient and Stable Electrocatalytic Water Splitting. *ChemNanoMat*, 2020, 6 , 1119 -1126.
6. J. M. Cen, L. Y. Wu, Y. F. Zeng, A. Ali, Y. Q. Zhu, P. K. Shen, Heterogeneous NiFeCoP/NF Nanorods as a Bifunctional Electrocatalyst for Efficient Water Electrolysis. *Chemcatchem* 2021, 12, 4602-4609.
7. D. L. Jiang, Y. Xu, R. Yang, D. Li, S. C. Meng, M. Chen, CoP₃/CoMoP Heterogeneous Nanosheet Arrays as Robust Electrocatalyst for pH-Universal Hydrogen Evolution Reaction. *ACS* 2019, 7, 9309-9317.
8. M. Z. Liu, Z. Sun, S. Y. Li, X. W. Nie, Y. F. Liu, E. D. Wang, Z. K. Zhao, Hierarchical superhydrophilic/superaerophobic CoMnP/Ni₂P nanosheet-based microplate arrays for enhanced overall water splitting. *J. Materials Chemistry* 2021, 9, 22129-22139.
9. W. S. Mai, Q. Cui, Z. Q. Zhang, K. K. Zhang, G. Q. Li, L. H. Tian, W. Hu, CoMoP/NiFe-Layered Double-Hydroxide Hierarchical Nanosheet Arrays Standing on Ni Foam for Efficient Overall Water Splitting. *ACS. Applied* 2020, 3, 8075-8085.
10. M. Lu, L. Li, D. Chen, J. Li, N.I. Klyui, W. Han, MOF-derived nitrogen-doped CoO@CoP arrays as bifunctional electrocatalysts for efficient overall water splitting. *Electrochim. Acta*, 2020, 330, 135210.